Philosophical Magazine
2010, 1–13, iFirst

The edge effect in nanoindentation

Joseph E. Jakes[ab] and Donald S. Stone[ac]*

[a]*Materials Science Program, University of Wisconsin-Madison, Madison, Wisconsin, USA;* [b]*Performance Enhanced Biopolymers, United States Forest Service, Forest Products Laboratory, Madison, Wisconsin, USA; 'Department of Materials Science and Engineering, University of Wisconsin-Madison, Madison, Wisconsin, USA*

(Received 23 October 2009; final version received 19 May 2010)

Until recently, obtaining unambiguous data from a nanoindentation measurement placed near a free edge has not been possible because the discontinuity associated with the edge introduces artifacts into the measurement. The primary consequence of a free edge is to introduce a structural compliance, C_s, into the measurement. Like the machine compliance, C_m, C_s is independent of the size of the indent and it adds to the measured unloading compliance; but unlike C_m, C_s is a function of position. Accounting for C_s in nanoindentation analyses removes the artifacts in nanoindentation measurements associated with the edge, allowing researchers to more accurately probe material properties near an edge. Expressions were obtained for the effect of the free edge on hardness and modulus measured using the Oliver–Pharr method. The theory was tested on specimens including fused silica, poly(methyl methacrylate), and a layered silicon-on-insulator specimen.

Keywords: nanoindentation; edge effect

1. Introduction

A key capability of nanoindentation is its ability to probe local mechanical properties in specimens that are highly non-uniform. Determining how properties change near an edge, such as the interface between phases or a free edge, is often of interest. The problem with making those kinds of measurements is that, above and beyond any effect associated with changes in properties near the edge, the presence of the elastic discontinuity will itself give rise to effects, i.e. artifacts, that make the properties (hardness and modulus) appear to change even if the local properties remain uniform up to the edge. To increase the accuracy of nanoindentation measurements in highly non-uniform specimens, experimenters must be able to anticipate and account for these artifacts. Prior researchers have studied this problem using finite element simulations (e.g. [1,2]) and analytic modeling (e.g. [3–8]). However, those methods lack both theoretical and experimental convenience, and they do not provide a general way of assessing artifacts brought about by

*Corresponding author. Email: dsstone@wisc.edu

ISSN 1478–6435 print/ISSN 1478–6443 online
© 2010 Taylor & Francis
DOI: 10.1080/14786435.2010.495360
http://www.informaworld.com

complicated geometries. In previous articles [9,10], we have found a way to simplify the problem by demonstrating that a free edge or heterophase interface introduces a 'structural' compliance, C,, whose effects can be removed from the measurement.

In this paper, we provide experimenters using the Oliver–Pharr method of data analysis [11] a tool to anticipate when free edges will affect their measurements. Below, we numerically incorporate an adaptation of Gerber's theory for the elastic contact of a punch against an elastic quarter space [3] into the Oliver–Pharranalysis to predict the effect of a nearby free edge on the elastic modulus and hardness calculated using the Oliver–Pharranalysis. The numerical results are compared with measurements made using nanoindentation close to the free edges of fused silica (FS) and poly(methyl methacrylate) (PMMA). We also include data from a layered silicon-on-insulator (SOI) specimen to demonstrate that the theory is applicable to estimating the magnitude of the artifact near the edges of layered specimens. We demonstrate how the measurements of hardness and modulus, based on the Oliver–Pharr analysis, become altered in the presence of a nearby free edge, and we demonstrate how to correct the analysis to remove the errors.

2. Theory

2.1. *Standard Oliver–Pharr analysis*

With the Oliver–Pharmethod [11], the area of a nanoindent, A, is determined based on contact depth, h_c, defined as

$$h_c = h_0 - \varepsilon P_0 C_p, \tag{1}$$

where h_0 is the depth immediately prior to unloading, ε a geometric factor approximately equal to 0.75 for a Berkovich indenter, P_0 the load immediately prior to unloading, and C, the contact compliance, which is the compliance attributable to the indenter tip and specimen in a measurement made far from a free edge so that the artifacts caused by the edge are negligible. The area of the indent is calculated using h, in a calibrated area function $A(h_c)$. The Meyer hardness is

$$H = \frac{P_0}{A}. \tag{2}$$

The elastic properties of the specimen can be related to C_p according to

$$C_p = \frac{1}{E_{eff} A^{1/2}}, \tag{3}$$

where E_{eff} is an 'effective' modulus for contact. For indentation against a homogenous, isotropic, elastic half-space,

$$\frac{1}{E_{eff}} = \frac{1}{\beta}\left(\frac{1}{E_r} + \frac{1-\nu_d^2}{E_d}\right), \tag{4}$$

where E, represents the properties of the specimen and E_d and v_d are, respectively, the Young's modulus and Poisson's ratios of the indenter. For a uniform, isotropic specimen $E_r = E_s/(1 - v_s^2)$ where E_s and v_s are the specimen Young's modulus and

Poisson's ratio, respectively. For a layered specimen such as a thin film on substrate, E_r becomes a function of the size of the indent in relation to the layer thickness. β is a numerical factor, which is usually assumed to be $2/\pi^{1/2} = 1.128$ based on the approximation of the indenter as a flat, circular punch. Some authors [12–15] have reported that this value is too low and that the actual value is closer to 1.2. Finite element analysis simulations of cone indentation in rate-sensitive materials reveal that β ranges between 1.16 and 1.22 depending on hardness/modulus ratio [16]. At present, we find that $\beta \cong 1.23$ works best in experiments [9]; however, to be consistent with usual practice we employ $\beta = 1.128$ in the Oliver–Pharr-based calculations below. $\beta = 1.23$ is used for calculations of modulus that rely on directly measuring the areas of indents [9].

2.2. Corrected analysis accounting for structural compliance

A free edge gives rise to a structural compliance, C_s [9]. To accurately determine mechanical properties for indents placed near edges, C_s must be taken into account. The total measured compliance is $C_t = C_p + C_m + C_s$. If C_t is multiplied by $P_0^{1/2}$, then from Equations (2) and (3) it is shown [9,17] that

$$C_t P_0^{1/2} = (C_m + C_s) P_0^{1/2} + J_0^{1/2}, \tag{5}$$

where $J_0 = H/E_{eff}^2$ is the Joslin–Oliver[18] parameter. In the remainder of the paper, we assume for simplicity sake that the machine compliance, C_m, has already been removed from the experimental data and all that remains is the structural compliance, in which case,

$$C_t P_0^{1/2} = C_s P_0^{1/2} + J_0^{1/2}. \tag{6}$$

If J_0 is independent of load, then $C_t P_0^{1/2}$ plotted as a function of $P_0^{1/2}$ forms a straight line of slope C_s. If J_0 is a function of load, then the determination of C_s is less straightforward but can still be achieved. For example, with thin film specimens on substrates where most of the indentation size effect comes from the different elastic properties of the layers, it is possible to back out the effect using elasticity theory to model C_p as a function of the size of the indent [10]. After determining C, for a nanoindent, the corresponding load–depth trace can be corrected by subtracting the product PC_s, where P is the instantaneous load, from the depth.

2.3. Consequences of not accounting for structural compliance in Oliver–Pharr analysis

A structural compliance produces an error in the measurement of indenter depth, which in turn propagates into errors in contact stiffness and area. We denote the various quantities that have not been corrected for these errors with superscript u, for 'uncorrected'. The uncorrected contact depth is therefore

$$\begin{aligned} h_c^u &= h_0^u - \varepsilon P_0 (C_p + C_s) \\ &= h_c + (1 - \varepsilon) P_0 C_s, \end{aligned} \tag{7}$$

where $h_0^u = h_0 + P_0 C_s$ and h_c is substituted from Equation (1). For an ideal cone- or pyramid-shaped indenter, the contact area is

$$A = kh_c^2, \tag{8}$$

where $\boldsymbol{k}$ is a proportionality factor. Substituting h_c from Equation (8) and P_0 from Equation (2) into Equation (7), we have

$$h_c^u = A^{1/2}\left[\frac{1}{k^{1/2}} + (1-\varepsilon)HA^{1/2}C_s\right]. \tag{9}$$

Eliminating the factor $A^{1/2}$ inside the brackets from Equation (3) gives

$$h_c^u = A^{1/2}\left[\frac{1}{k^{1/2}} + (1-\varepsilon)\frac{H}{E_{eff}}\frac{C_s}{C_p}\right]. \tag{10}$$

Finally, substituting this formula back into the area function we obtain the 'uncorrected' area,

$$A^u = A\left[1 + (1-\varepsilon)k^{1/2}\frac{H}{E_{eff}}\frac{C_s}{C_p}\right]^2. \tag{11}$$

This expression represents the value of the area calculated from the load–depth trace using the Oliver–Pharr approach when there is a structural compliance that is not properly accounted for in the analysis. Near a free edge, $C_s > 0$, so the uncorrected area is larger than the actual area. The uncorrected hardness is calculated as

$$H^u = \frac{P_0}{A^u} = \frac{H}{\left[1 + (1-\varepsilon)k^{1/2}\frac{H}{E_{eff}}\frac{C_s}{C_p}\right]^2} \tag{12}$$

Similarly, the uncorrected effective modulus is

$$E_{eff}^u = \frac{E_{eff}}{\left(1 + \frac{C_s}{C_p}\right)\left[1 + (1-\varepsilon)k^{1/2}\frac{H}{E_{eff}}\frac{C_s}{C_p}\right]} \tag{13}$$

2.4. *Theory for free edge*

Gerber [3] worked on some problems in elastic contact between a square, rigid punch and an elastic quarter space (Figure 1). Jakes et al. [9] analyzed Gerber's results in context of King's [19] solution for indentation of an elastic half-space to arrive at an estimate of the structural compliance caused by a free edge as

$$C_s = \frac{0.20 + 0.11\nu_s}{E_s d} = \frac{(0.20 + 0.11\nu_s)\beta}{1-\nu_s^2}\frac{1}{E_{eff}d}, \tag{14}$$

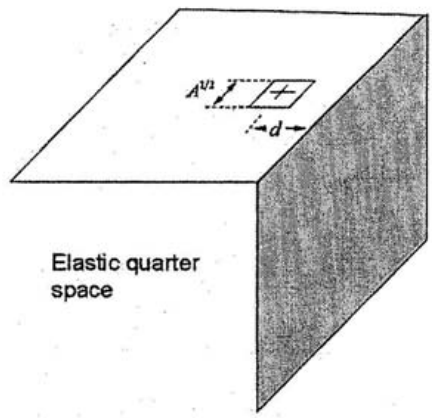

Figure 1. Geometry of the edge problem solved by Gerber [3] and reanalyzed by Jakes et al. [9] to provide an estimate for the structural compliance in the form of Equation (14). The structural compliance is independent of the size of the indent (i.e. $A^{1/2}$) but depends on the distance from the center of the indent to the free edge (d).

where d is the distance from the edge to the center of the indent. Substituting Equation (14) into Equation (11) and using Equation (3), we have

$$A^{\mathrm{u}} = A\left[1 + (1-\varepsilon)k^{1/2}\frac{(0.20+0.11\nu_{\mathrm{s}})\beta}{1-\nu_{\mathrm{s}}^2}\frac{H}{E_{\mathrm{eff}}}\frac{A^{1/2}}{d}\right]^2. \tag{15}$$

Similarly,

$$H^{\mathrm{u}} = \frac{H}{\left[1 + (1-\varepsilon)k^{1/2}\frac{(0.20+0.11\nu_{\mathrm{s}})\beta}{1-\nu_{\mathrm{s}}^2}\frac{H}{E_{\mathrm{eff}}}\frac{A^{1/2}}{d}\right]^2} \tag{16}$$

and

$$E_{\mathrm{eff}}^{\mathrm{u}} = \frac{E_{\mathrm{eff}}}{\left(1 + \frac{(0.20+0.11\nu_{\mathrm{s}})\beta}{1-\nu_{\mathrm{s}}^2}\frac{A^{1/2}}{d}\right)\left[1 + (1-\varepsilon)k^{1/2}\frac{(0.20+0.11\nu_{\mathrm{s}})\beta}{1-\nu_{\mathrm{s}}^2}\frac{H}{E_{\mathrm{eff}}}\frac{A^{1/2}}{d}\right]}. \tag{17}$$

According to this analysis, errors in hardness and modulus depend on three dimensionless parameters: the size of the indent in relation to the distance to the edge $(A^{1/2}/d)$, the hardness/modulus ratio (H/E_{eff}), and the Poisson's ratio (ν_{s}).

Figures 2-4 show the predicted effects using values of $k = 24.5$, $\beta = 1.128$, and $\varepsilon = 0.75$. For materials with small H/E_{eff}, the predicted errors in A and H are small. The error in E_{eff} remains important even for low H/E_{eff} materials.

3. Experimental

Experiments were performed on PMMA, FS, and SOI to compare edge effects on measurements of hardness with the theory represented by Equations (16) and (17).

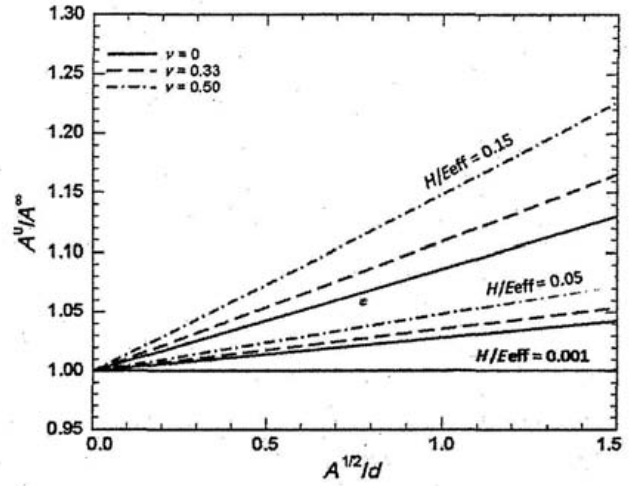

Figure 2. The theoretical effect of the size of the indent in relation to the distance to the edge $(A^{1/2}/d)$, the hardness/modulus ratio (H/E_{eff}), and the Poisson's ratio (ν_s) on the area determined by the Oliver–Pharr method if the structural compliance caused by the free edge is not taken into account. The curves are calculated using Equation (15).

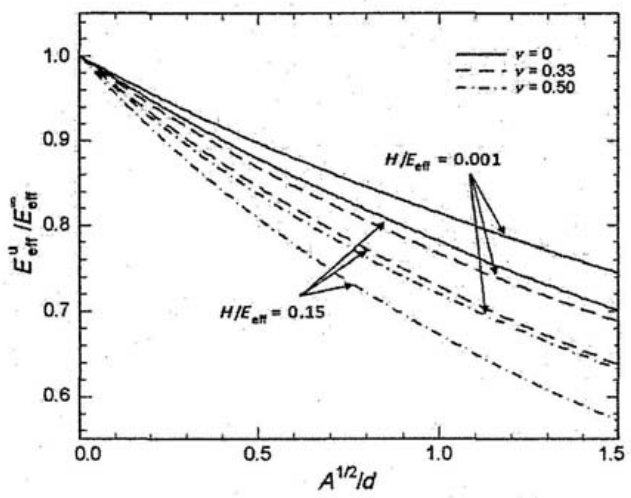

Figure 3. The theoretical effect of the size of the indent in relation to the distance to the edge $(A^{1/2}/d)$, the hardness/modulus ratio (H/E_{eff}), and the Poisson's ratio (ν_s) on the modulus determined by the Oliver–Pharr method if the structural compliance caused by the free edge is not taken into account. The curves are calculated using Equation (17).

The experimental methods have been described elsewhere [9,10], but some of the salient details are repeated here.

The PMMA specimen was obtained as a 3.33 mm diameter extruded rod (density 1.15 g/cm^3) from Cope Plastics, Inc. (Godfrey, Illinois, USA). A 3 mm long cylinder was removed from the end for testing and cross-sectioned perpendicular to the

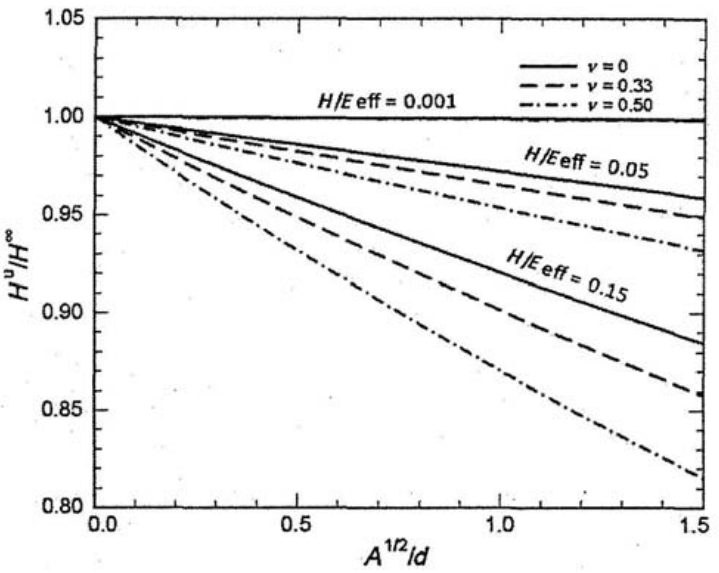

Figure 4. The theoretical effect of the size of the indent in relation to the distance to the edge ($A^{1/2}/d$), the hardness/modulus ratio (H/E_{eff}), and the Poisson's ratio (ν_s) on the hardness determined by the Oliver–Pharrmethod if the structural compliance caused by the free edge is not taken into account. The curves are calculated using Equation (16).

extrusion direction using an ultramicrotome fit with a diamond knife. Next, a free edge was created by cutting the cylinder in half at 90° to the testing surface using an ultramicrotome fit with a glass knife. Experiments were performed near the freshly cut edge.

The FS was a calibration standard obtained from Hysitron (Minneapolis, Minnesota, USA). A location was found along the perimeter of the specimen where the edges appeared sharp and perpendicular, and at this location indents were placed at various distances from the edge.

Last, a relaxed SOI specimen prepared through SMART CUT^{TM} technology was used for the third set of experiments [20]. The specimen consists of a 65 nm thick relaxed silicon layer on top of an insulating, 149 nm thick silicon oxide layer, which is deposited on top of a 525 µm thick silicon wafer of (1 00) orientation. The thicknesses of the two top layers were measured by a Woollam (Lincoln, Nebraska, USA) ellipsometer. Further details about this specimen are given by Miller et al. [20]. In the analysis of this specimen, elasticity theory was used to model the effects of the different layers on measured stiffness [21]. Some of the indents were placed near the free edge of the specimen to examine the combined effects of layers and free edge. The free edge was prepared by cleaving the specimen along a (100) surface.

A Hysitron (Minneapolis, Minnesota, USA) Triboindenter was used to perform the experiments. The nanoindenter was equipped with a Berkovich tip, and standard methods were used to calculate the machine compliance and area function (based on contact stiffness) using a series of indents in the center of the fused silica standard.

Residual indents were imaged with a Quesant (Agoura Hills, California, USA) atomic force microscope (AFM) incorporated in the Triboindenter. AFM images allow us to measure the areas of indents and the distances from the center of the indents to the free edge of the specimens. The AFM was operated in contact mode. For accurate distance and area measurements, the AFM was calibrated using an Advanced Surface Microscopy, Inc. (Indianapolis, Indiana, USA) calibration standard with a pitch of 292 ± 0.5 nm. Successive scans and calibration routines revealed the reproducibility of the AFM calibration to be ±1%.

Structural compliance was determined by measuring the unloading compliance as a function of load using multi-load indents and then using Equation (6). Details for the procedure are given in [9] for FS and in [10] for PMMA and SOI. It is important to recognize that both viscoelastic and viscoplastic deformation can affect the unloading slope [22–28], especially in glassy polymers like PMMA; and for this reason the load-hold-unload profile must be chosen carefully to exclude artifacts arising from rate effects. For instance, if we were to use loading ramps with constant rate of load (P) or displacement (h), independent of load in the multi-load experiment, this would cause both the hardness and modulus to appear to decrease at higher loads because the strain rates at higher loads are lower. To perform experiments at fixed P or h would thereby lead to confusion in the measurement of structural compliance. A way to get around this problem is to rely on fixed loading, hold, and unloading times, independent of load [9,10]. For all experiments, the final maximum load was 10 mN.

For FS and PMMA, which have no indentation size effect, C_s can be obtained from the slope of a plot of $C_t P_0^{1/2}$ vs. $P_0^{1/2}$. For SOI there is an indentation size effect; however, it is still possible to determine the structural compliance by comparing $CtP_0^{1/2}$ vs. $P_0^{1/2}$ obtained near the edge with those obtained far from the edge [10].

Hardness and modulus determined using the Oliver–Pharr method on indents far from the edge are shown in Table 1 along with the values of Poisson's ratio necessary to calculate E_s. For SOI, which is a layered specimen, $\nu_s = 0.22$ was chosen to fall in between that of FS and silicon ($\nu_s = 0.28$ [29]). The vast majority of experimenters employ $ß = 1.128$ when using the Oliver–Pharr method, so we did the same here. In order to verify whether the properties change near the edge, it is necessary to measure the areas directly. For this reason Table 1 also includes the values of hardness and modulus obtained using direct area measurements. These values are taken from our previous work [9,10], in which case $ß = 1.23$ is used to calculate E_s from E_{eff}. Our previously reported values of modulus and hardness from the Oliver–Pharr method are different from the values in Table 1 because in that work we also used $ß = 1.23$ in the Oliver–Pharr method. However, these differences are not important to the problem at hand because comparisons between the two methods (see Figures 8 and 9) rely on relative changes in measured properties, which are not sensitive to these differences.

4. Results and discussion

The modulus and hardness were calculated using the Oliver–Pharr analysis of load–depth traces uncorrected for C_s. The results of these measurements are plotted

Table 1. H^{∞}, $E_{\mathrm{eff}}^{\infty}$, E_{s}^{∞}, and ν_{s} for experimental materials.

	Oliver–Pharr			Direct area measurement			
Material	H^{∞} (GPa)	$E_{\mathrm{eff}}^{\infty}$ (GPa)	E_{s}^{∞} (GPa)	H^{∞} (GPa)	$E_{\mathrm{eff}}^{\infty}$ (GPa)	E_{s}^{∞} (GPa)	ν_{s}
FS	9	77	71	11	86	72	0.17 [11]
PMMA	0.22	6.1	4.8	0.28	7.1	5.1	0.35 [30]
SOI	11	140	130	12	150	130	0.22

Note: $^{\infty}$ denotes property values obtained far from the edge.

against distance from the center of the indent to the edge in Figure 5. All the properties appear to decrease as the edge is approached, although the effect is largest in the modulus.

Results are compared with theory in Figures 6 and 7, in which $E_{\mathrm{eff}}^{\infty}$ and H^{∞} have been taken to represent the properties in absence of an edge effect. The data are consistent with theory.

We obtain the corrected values of modulus and hardness by determining the corrected depth (h^{c}) by subtracting from the uncorrected depth, h^{u}, the effect attributed to structural compliance,

$$h^{\mathrm{c}} = h^{\mathrm{u}} - C_{\mathrm{s}}P, \tag{18}$$

and h^{c} is then used as the basis for reanalyzing the data employing the Oliver–Pharr method. The results of the 'corrected' modulus and hardness, designated $E_{\mathrm{eff}}^{\mathrm{c}}$ and H^{c}, respectively, are shown in Figures 8 and 9 as open symbols. The closed symbols are obtained by directly measuring the areas of the indents using AFM. It is seen that the moduli can be accurately measured as close to the edge as $\sqrt{A}/d = 1.3$. The FS hardness can also be measured this close to the edge; but the PMMA hardness is seen to decrease when $\sqrt{A}/d > 0.6$. This effect does not appear to be an artifact, because it is seen using both the corrected Oliver–Pharr analysis and by measuring the areas directly from AFM images. One possible origin of this effect is the proximity of the plastic zone to the edge.

Because PMMA has a lower H/E_{eff} ratio than fused silica, the radius of the plastic zone (r_p) of PMMA is larger [31–33] and therefore likely to reach the edge sooner than the plastic zone for FS. However, a preliminary analysis suggests that the problem of predicting when the edge will affect the hardness might not be a straight forward one. Figure 5 in Reference [33] can be used to estimate the radius of the plastic zone. For FS the closest indent has an r_p/d value of about 0.95, suggesting that the plastic zone should just touch the edge. For PMMA the indent where the hardness begins to drop is at $r_p/d \approx 0.55$. Based on this simple argument, therefore, the edge should affect FS more than it does PMMA, which seems to contradict our results. Nevertheless, it is likely that other factors in addition to r_p/d also come into play including the rate- and pressure-sensitivity of yielding along with the ratio $\sqrt{A}/d$. In the SOI, the indent placed closest to the edge (designated by arrows in Figures 6–9) caused fracture during loading. We were nevertheless able to analyze the data from this indent and have included it in the figures.

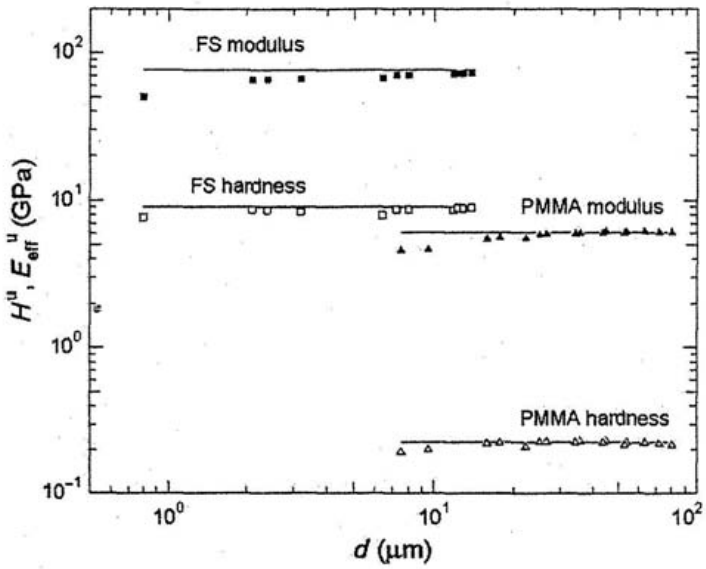

Figure 5. Measured effects of the edge on (apparent or uncorrected) hardness and modulus. d is the distance from the center of the indent to the edge. For comparison, $\sqrt{A} \approx 0.95$ μm for the indents in FS, and $\sqrt{A} \approx 6$ μm in PMMA.

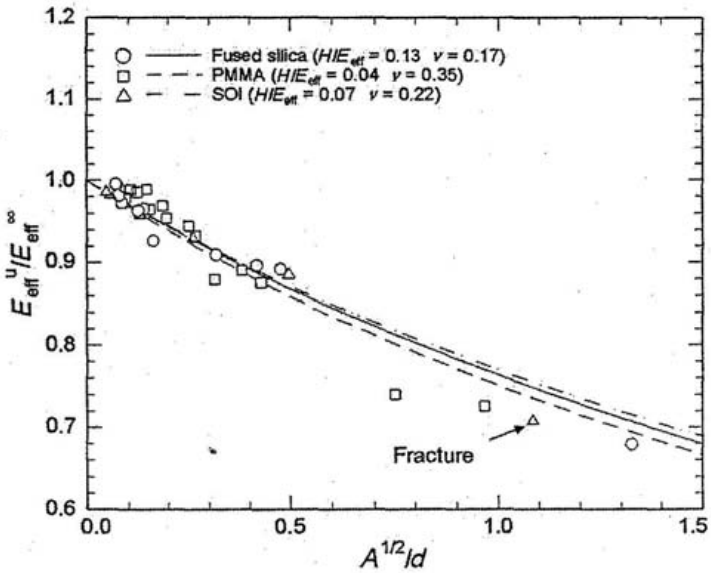

Figure 6. Experimentally measured effect of edge proximity on 'uncorrected' modulus (symbols) compared with theory (lines). E_{eff}^{∞} is the measured modulus determined by the Oliver–Pharr method far from the edge (Table 1). The theory lines are from Equation (17) with values of k = 24.5, $ß$ = 1.128, and ε = 0.75. The SOI indent placed closest to the edge fractured, which affected the datum.

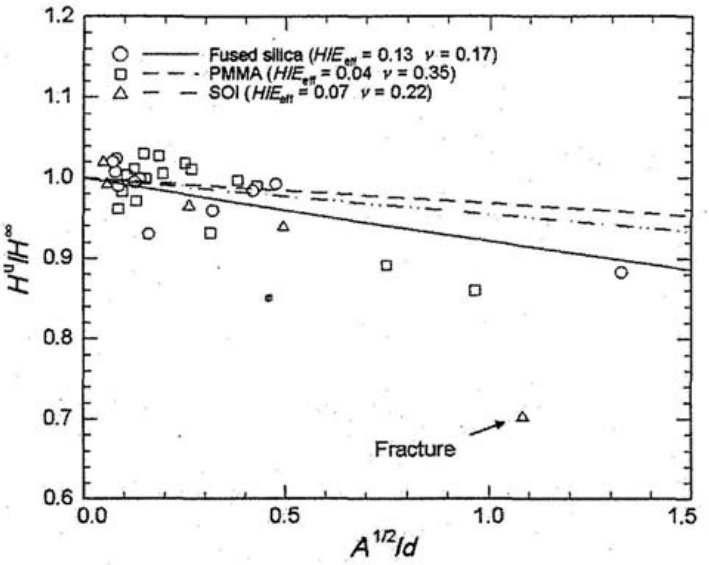

Figure 7. Experimentally measured effect of edge proximity on 'uncorrected' hardness (symbols), compared with theory (lines). H^{∞} is the measured hardness determined by the Oliver–Pharrmethod far from the edge (Table 1). The theory lines are from Equation (16) with values of $k = 24.5$, $\beta = 1.128$, and $\varepsilon = 0.75$. The SOI indent placed closest to the edge fractured, which affected the datum.

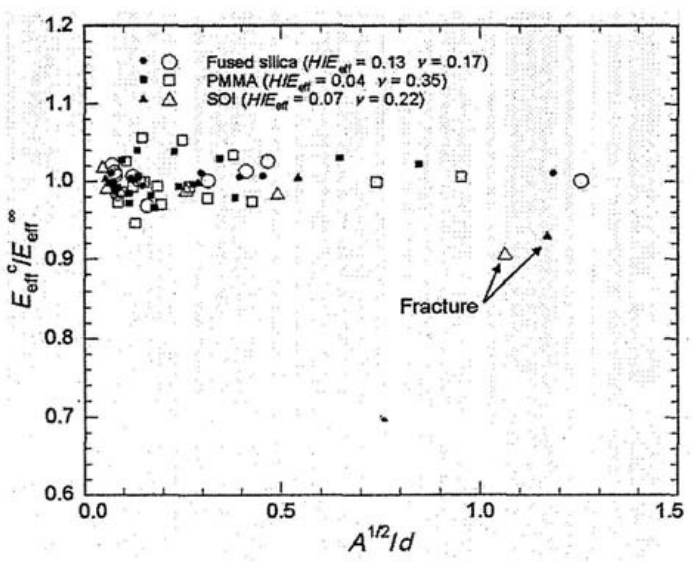

Figure 8. (Open symbols) Modulus values determined using the Oliver–Pharr method after the depth has been corrected for the structural compliance. (Closed symbols) Modulus values determined using the corrected depth and direct area measurement following the procedures of Jakes and coworkers [9,10]. E_{eff}^{∞} is the measured modulus determined far from the edge (Table 1). The SOI indent placed closest to the edge fractured, which affected the datum.

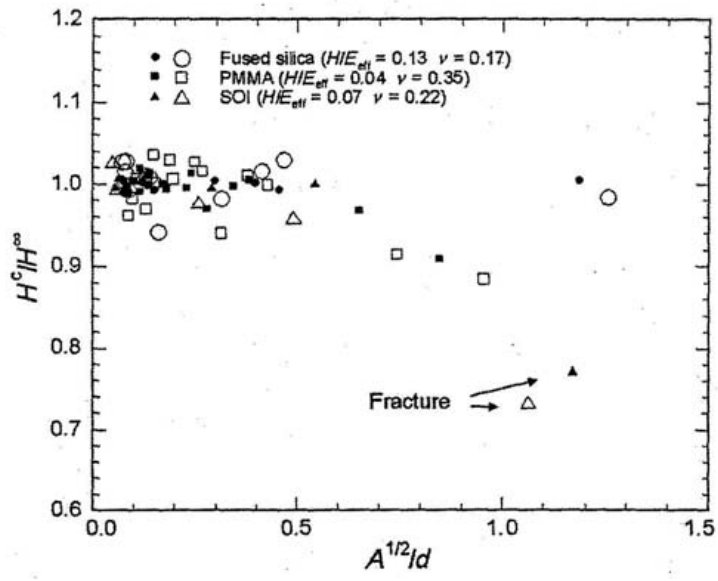

Figure 9. (Open symbols) Hardness values determined using the Oliver–Pharr method after the depth has been corrected for the structural compliance. (Closed symbols) Hardness values determined using the corrected depth and direct area measurement following the procedures of Jakes and coworkers [9,10]. H^∞ is the measured hardness determined far from the edge (Table 1). The SOI indent placed closest to the edge fractured, which affected the datum.

5. Summary

The presence of a nearby edge will affect a nanoindentation measurement. Part of the effect arises from the way the experiment is analyzed. The artifact manifests in terms of a structural compliance, the magnitude of which is inversely proportional to the distance to edge. The structural compliance can be measured, and the artifact caused by it can be removed so that corrected modulus and hardness values are obtained. We are able to account for the magnitude of this artifact based on the theory of Gerber [3] for the stiffness of contact between a punch and an elastic quarter space.

When indents are placed sufficiently close to the edge, the hardness decreases. We believe this effect is real, in the sense that a true decrease in pressure is required to plastically deform a material near the edge where constraint of the plastic zone is lost. The effect is seen in PMMA for indents closer than $d < \sqrt{A}/0.6$, but is not seen in FS for indents placed as close as $d = \sqrt{A}/1.3$.

Acknowledgements

D.S. Stone wishes to acknowledge support by the National Science Foundation under Grant Nos. DMR 0351449 (PREM Program) and DMR 0520527 (MRSEC Program). The authors would like to thank A.A. Elmustafa and H. Baumgart for supplying the SOI specimen.

References

[1] B.J.F. Bruet, S. Juha, M.C. Boyce and C. Ortiz, Nat. Mater. 7 (2008) p.748.
[2] S.-H. Lee, S. Wang, G.M. Pharr and H. Xu, Compos. Appl. Sci. Manuf. 38 (2007) p.1517.
[3] C.E. Gerber, *Contact Problems for the Elastic Quarter-Plane and for the Quarter Space*, Stanford University, Palo Alto, 1968, p. 100.
[4] N. Schwarzer, I. Hermann, T. Chudoba and F. Richter, Surf. Coating Tech. 146–147 (2001) p.371.
[5] M. Hetenyi, J. Appl. Mech. 27 (1960) p.289.
[6] M. Hetenyi, J. Appl, Mech. 37 (1970) p.70.
[7] L.M. Keer, J.C. Lee and T. Mura, Int. J. Solid Struct. 20 (1984) p.513.
[8] G.Y. Popov, Mech. Solid 38 (6) (2003) p.23.
[9] J.E. Jakes, C.R. Frihart, J.F. Beecher, R.J. Moon and D.S. Stone, J. Mater. Res. 23 (2008) p.1113.
[10] J.E. Jakes, C.R. Frihart, J.F. Beecher, R.J. Moon, P.J. Resto, Z.H. Melgarejo, O.M. Surez, H. Baumgart, A.A. Elmustafa and D.S. Stone, J. Mater. Res. 24 (2009) p.1016.
[11] W.C. Oliver and G.M. Pharr, J. Mater. Res. 7 (1992) p.1564.
[12] A.C. Fischer-Cripps, Surf. Coating Tech. 200 (2006) p.4153.
[131 W.C. Oliver and G.M. Pharr, J. Mater. Res. 19 (2004) p.3.
[14] M. Troyon and S. Lafaye, Phil. Mag. 86 (2006) p.5299.
[15] Y.-T. Cheng and C.-M. Cheng, Materials Sci. Eng. R 44 (2004) p.91.
[16] A.A. Elmustafa, S. Kose and D.S. Stone, J. Mater. Res. 22 (2007) p.926.
[17] D.S. Stone, K.B. Yoder and W.D. Sproul, J. Vac. Sci. Tech. A 9 (1991) p.2543.
[18] D.L. Joslin and W.C. Oliver, J. Mater. Res. 5 (1990) p.123.
[19] R.B. King, Int. J. Solid Struct. 23 (1987) p.1657.
[20] N. Miller, K. Tapily, H. Baumgart, G.K. Cellar, F. Brunier and A.A. Elmustafa, *Nanomechanical properties of strained silicon-on-insulator (SOI) films epitaxially grown on Sil-xGex and layer transferred wafer bonding*, in *Proceedings of the Materials Research Society*, San Fransisco, CA, 2007.
[21] D.S. Stone, J. Mater. Res. 13 (1998) p.3207.
[22] B.J. Briscoe, L. Fiori and E. Pelillo, J. Phys. D Appl. Phys. 31 (1998) p.2395.
[23] G. Feng and A.H.W. Ngan, J. Mater. Res. 17 (2002) p.660.
[24] N. Fujisawa and M.V. Swain, J. Mater. Res. 21 (2006) p.708.
[25] N. Fujisawa and M.V. Swain, J. Mater. Res. 23 (2008) p.637.
[26] A.H.W. Ngan and B. Tang, J. Mater. Res. 17 (2002) p.2604.
[27] A.H.W. Ngan, H.T. Wang, B. Tang and K.Y. Sze, Int. J. Solid Struct. 42 (2005) p.1831.
[28] Y.-T. Cheng and C.-M. Cheng, J. Mater. Res. 20 (2005) p.1046.
[29] R. Hull, *Properties of Crystalline Silicon*, IEE, 1999, pp.xxvi+1016.
[30] R. Kono, J. Phys. Soc. Jpn. 15 (1960) p.718.
[31] S.S. Chiang, D.B. Marshall and A.G. Evans, J. Appl. Phys. 53 (1982) p.298.
[32] K.L. Johnson, *Contact Mechanics*, Cambridge University Press, Cambridge, UK, 1985, p.452.
[33] J. Chen and S.J. Bull, Surf. Coating Tech. 201 (2006) p.4289.

This article was downloaded by: *[Stone, Donald S.]*
On: *13 July 2010*
Access details: *Access Details: [subscription number 923829247]*
Publisher *Taylor &Francis*
Informa Ltd Registered in England and Wales Registered Number: 1072954 Registered office: Mortimer House, 37-41 Mortimer Street, London W1T 3JH, UK

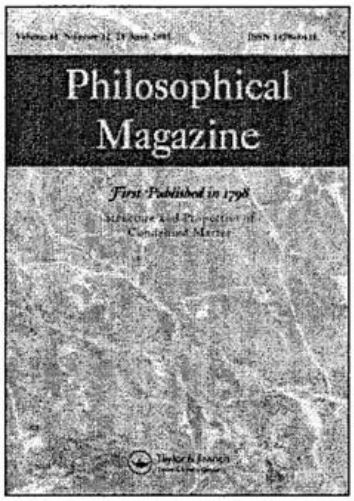

Philosophical Magazine
Publication details, including instructions for authors and subscription information:
http://www.informaworld.com/smpp/title~content=t713695589

The edge effect in nanoindentation

Joseph E. Jakes[ab]; Donald S. Stone[ac]
[a] Materials Science Program, University of Wisconsin-Madison, Madison, Wisconsin, USA [b] Performance Enhanced Biopolymers, United States Forest Service, Forest Products Laboratory, Madison, Wisconsin, USA [c] Department of Materials Science and Engineering, University of Wisconsin-Madison, Madison, Wisconsin, USA

First published on: 05 July 2010

To cite this Article Jakes, Joseph E. and Stone, Donald S. (2010) 'The edge effect in nanoindentation', Philosophical Magazine,, First published on: 05 July 2010 (iFirst)
To link to this Article: DOI: 10.1080/14786435.2010.495360
URL: http://dx.doi.org/10.1080/14786435.2010.495360

Sign on

SAO/NASA ADS General Science Abstract Service

• **Find Similar Abstracts (with default settings below)**

• **Translate This Page**

Title: The edge effect in nanoindentation

Authors: Jakes, Joseph; Stone, Donald

Publication: Philosophical Magazine, vol. 91, issue 7-9, March 2011, pp. 1387-1399

Publication Date: 03/2011

Origin: CROSSREF

DOI: 10.1080/14786435.2010.495360

Bibliographic Code: 2011PMag...91.1387J